



ORIGINAL ARTICLE

Synthesis, characterization, and miRNA-mediated PI3K suppressing activity of novel cisplatin-derived complexes of selenones



Homood M. As Sobeai^a, Adam A. A. Sulaiman^b, Saeed Ahmad^c,
Abdul Rajjak Shaikh^d, Ridwan Sulaimon^e, Moureq R. Alotiabi^a,
Fahad AlZoghaibi^f, Ali Osman Altoum^c, Anvarhusein A. Isab^e, Ali R. Alhoshani^{a,*}

^a Pharmacology and Toxicology Department, College of Pharmacy, King Saud University, Riyadh 11451, Saudi Arabia

^b Lab Technical Support Office (LTSO), King Fahd University of Petroleum and Minerals, Dhahran 31261, Saudi Arabia

^c Department of Chemistry, College of Sciences and Humanities, Prince Sattam bin Abdulaziz University, Al-Kharj 11942, Saudi Arabia

^d KAUST Catalysis Center (KCC), Physical Sciences and Engineering Division (PSE), King Abdullah University of Science and Technology (KAUST), Thuwal 23955-6900, Saudi Arabia

^e Department of Chemistry, King Fahd University of Petroleum and Minerals, Dhahran 31261, Saudi Arabia

^f Molecular BioMedicine Program, Research Center, Faisal Specialist Hospital & Research Center, Riyadh 11211, Saudi Arabia

Received 7 April 2021; accepted 30 May 2021

Available online 4 June 2021

KEYWORDS

Cisplatin;
Selenones;
Spectroscopy;
Anti-cancer agents;
Docking;
Microarray;
miRNAs;
PI3K;
Apoptosis

Abstract New therapeutic options are crucially for most cancers, particularly those with poor clinical outcomes. Five new derivatives of cisplatin-containing selenone ligands with the general formula, *cis*-[Pt(NH₃)₂(Selenone)₂](NO₃)₂ (1–5) were synthesized and characterized using elemental analysis, Infrared, and nuclear magnetic resonance (¹H, ¹³C & ⁷⁷Se) spectroscopy. Spectroscopic and computational data supported the coordination of selenones to platinum(II). The structures of the complexes were predicted using density functional theory calculations. Molecular docking studies were carried out using the AutoDock Tools docking program. The *in vitro* cytotoxicity of these complexes and cisplatin against three human cancer cell lines, HeLa, A549, and HCT116 was investigated using the MTT assay. The best candidate complex, complex 3, was subjected to mechanistic assessments, including miRNA profiling, PI3K deactivation, and induction of apoptosis. Docking studies showed that all the newly synthesized platinum(II) complexes interacted with the minor DNA groove. The synthesized complexes showed promising cytotoxic effects against the

* Corresponding author.

E-mail address: ahoshani@ksu.edu.sa (A.R. Alhoshani).

Peer review under responsibility of King Saud University.



tested cell lines. Complex 3 modulated the miRNA expression signature in A549 cells. Pathway enrichment analyses of differentially expressed miRNA gene targets identified the PI3K/AKT signaling pathway as a promising target. Complex 3 inhibited PI3K activity and induced apoptosis. Collectively, our study identified promising new platinum(II) derivatives such as complex 3, paving the way for future *in vitro* and *in vivo* validations and safety studies.

© 2021 The Authors. Published by Elsevier B.V. on behalf of King Saud University. This is an open access article under the CC BY-NC-ND license (<http://creativecommons.org/licenses/by-nc-nd/4.0/>).

1. Introduction

Cisplatin, *cis*-diamminedichloridoplatinum(II) is one of the chemotherapeutic agents most commonly used for the treatment of several malignancies, including testicular, bladder, lung, and ovarian cancers (Ahmad, 2017; Dasari and Bernard Tchounwou, 2014a; Dilruba and Kalayda, 2016; Fennell et al., 2016; Ho et al., 2016; Johnstone et al., 2016; Kelland, 2007; Lovejoy and Lippard, 2009; Wheate et al., 2010; Wilson and Lippard, 2014). Despite the remarkable success of cisplatin in cancer treatment, its use is limited by two major factors: (i) its toxic side effects, especially nephrotoxicity, neurotoxicity, ototoxicity, and gastrointestinal toxicity (Dasari and Bernard Tchounwou, 2014a; Florea and Büsnelberg, 2011; Oun et al., 2018; Piccolini et al., 2013) and (ii) ineffectiveness against common human tumors such as colon and non-small cell lung cancers due to drug resistance (Florea and Büsnelberg, 2011; Galluzzi et al., 2012; Shen et al., 2012; Stewart, 2007; Zisowsky et al., 2007). These limitations emphasize the need for the identification of new platinum complexes with fewer side effects and with the capacity to overcome resistance (Bai et al., 2017; Deo et al., 2018; Dilruba and Kalayda, 2016; Galanski et al., 2005; Kelland et al., 1999; Lebowl and Canetta, 1998; Lovejoy and Lippard, 2009; Reedijk, 2009; Štarha et al., 2017; Wheate et al., 2010; Wilson and Lippard, 2014). Several derivatives of cisplatin, carboplatin, and oxaliplatin have been synthesized and tested for anti-tumor activity (Bai et al., 2017; Bernhardt et al., 2004; Carland et al., 2006; Chopade et al., 2015; Deo et al., 2018; Escibano et al., 2013; Fuks et al., 2010; Gay et al., 2015; Intini et al., 2017; Jomaa et al., 2019; Kelland et al., 1999; Kovala-Demertzi et al., 2009; Křikavová et al., 2016; Marverti et al., 2008; Miles et al., 2016; Pracharova et al., 2015; Štarha et al., 2017, 2010; Sun et al., 2012; Tamasi et al., 2010; Tian and He, 2015; Yin et al., 2011; Zeng et al., 2014). A few of these derivatives contain selenoether ligands such as selenomethionine (Carland et al., 2006; Chopade et al., 2015; Zeng et al., 2014). Selenium-containing compounds have been exploited in an effort to reduce the toxicity of platinum drugs because selenomethionine has been shown to reduce the renal toxicity of cisplatin in rats and mice. In this regard, we recently reported the synthesis, characterization, and antitumor properties of various platinum(II) complexes of selenones including [Pt(Selenone)₂Cl₂] (Altoum et al., 2017a), [Pt(Selenone)₄Cl₂] (Ahmad et al., 2018; Altoum et al., 2017b), and transplatin derivatives, *trans*-[Pt(NH₃)₂(Selenone)₂](NO₃)₂ (Alhoshani et al., 2019).

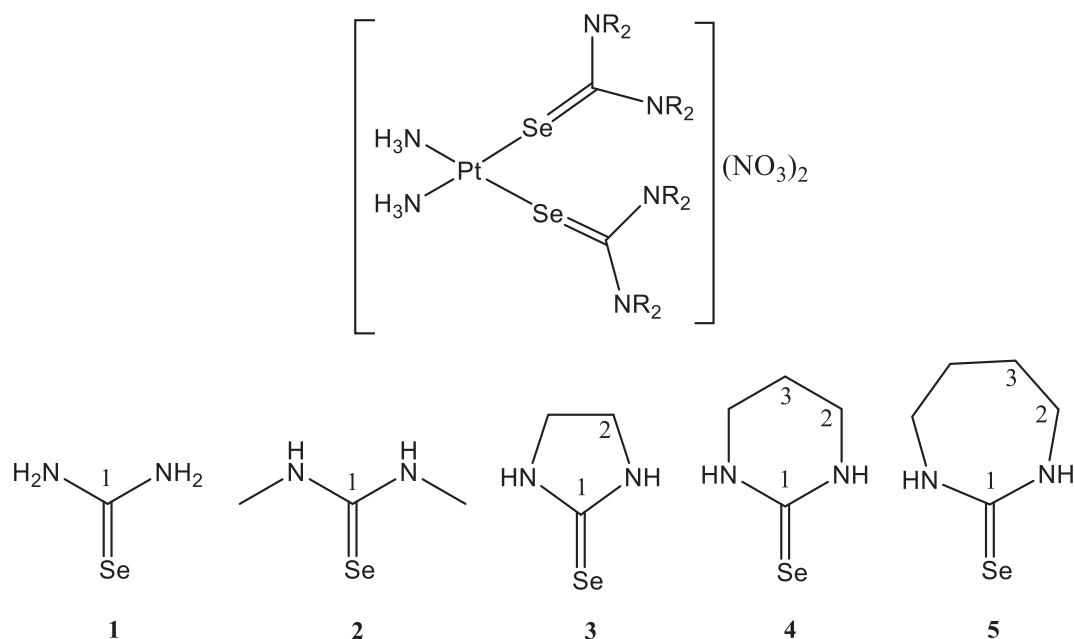
Lung cancer is the deadliest form of malignancy worldwide (Siegel et al., 2021; Sung et al., 2021). More than 50% of

patients with lung cancer in the United States succumb to the disease in the first year of diagnosis (Noone et al., 2018). Non-small-cell lung carcinoma (NSCLC) accounts for 84% of all lung cancer cases (American Cancer Society, 2021). Although NSCLC has a better prognosis than other types of lung cancers, small-cell lung carcinoma still has a poor overall prognosis with a 5-year relative survival rate of 25% (American Cancer Society, 2021). Thus, screening for new effective agents against NSCLC tumors is warranted.

MicroRNAs (miRNAs) are small (19-21 nucleotides) inhibitory non-coding RNAs that regulate gene expression post-transcriptionally by binding to a seed match located at the 3'-UTR of target mRNA (Bartel, 2004; Catalanotto et al., 2016; Jonas and Izaurralde, 2015). miRNAs are thought to target up to one-third of all known human mRNAs (Shu et al., 2017; Zhong et al., 2012). In fact, one miRNA can target hundreds of genes simultaneously (Schirle et al., 2014). Dysregulation of miRNAs has been reported in the majority of cancers, including lung cancer, and has been implicated in numerous oncogenic features such as proliferation, invasion, metastasis, angiogenesis, lack of apoptosis, and therapy resistance (Jansson and Lund, 2012; Kurozumi et al., 2016; Peng and Croce, 2016; Si et al., 2019; Singh and Mo, 2013). These features make miRNA regulation an appealing molecular process to investigate and understand the mechanisms through which newly proposed anti-cancer therapeutic agents function.

Considering that cisplatin-derived complexes may be more effective anti-cancer agents than cisplatin, we report newly synthesized novel complexes of selenone ligands with the general formula, *cis*-[Pt(NH₃)₂(Selenone)₂](NO₃)₂ that exhibited a promising tumor-suppressive activity. We described the synthesis, spectroscopic characterization, density functional theory (DFT)-optimized structures of these complexes. In addition, a molecular docking technique was used to analyze the interaction between these compounds and DNA and compared it with inhibitor activities obtained from experimental studies. Finally, functional and mechanistic investigations were conducted for the most promising complex out of the five new derivatives. This study provides a basis for future investigations and validations of cisplatin-derived selenone complexes. The structures of the selenone ligands are shown in Fig. 1.

- 1) Selenourea (Seu) (Complex 1)
- 2) *N,N'*-dimethylselenourea (Me₂Seu) (Complex 2)
- 3) 1,3-Imidazolidine-2-selenone (ImSe) (Complex 3)
- 4) 1,3-Diazinane-2-selenone (DiazSe) (Complex 4)
- 5) 1,3-Diazepane-2-selenone (DiapSe) (Complex 5)



- 1) Selenourea (Seu) (Complex 1)
- 2) *N,N'*-dimethylselenourea (Me₂Seu) (Complex 2)
- 3) 1,3-Imidazolidine-2-selenone (ImSe) (Complex 3)
- 4) 1,3-Diazinane-2-selenone (DiazSe) (Complex 4)
- 5) 1,3-Diazepane-2-selenone (DiapSe) (Complex 5)

Fig. 1 Structures of selenones used in this study.

2. Materials and methods

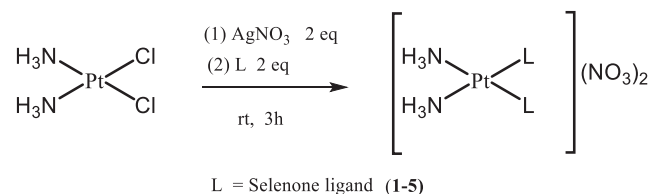
2.1. Chemicals

Cisplatin (*cis*-diamminedichloridoplatinum(II)) was obtained from Strem Chemicals, Inc. (Newburyport, MA, USA). Dimethyl sulfoxide-*d*₆ was purchased from Fluka® Analytical (Buchs, Switzerland). Selenourea and *N,N'*-dimethylselenourea were obtained from Acros Organics (Fair Lawn, NJ, USA). The other selenone ligands were prepared as described previously (Cristiani et al., 1977; Wazeer et al., 2003). (3-(4,5-Dimethylthiazol-2-yl)-2,5-diphenyltetrazolium bromide, a yellow tetrazole) was purchased from Sigma-Aldrich (St. Louis, MO, USA). The cancer cell lines, A549 (lung), HeLa (cervical), and HCT116 (colon) were purchased from the American Type Culture Collection (Manassas, VA, USA).

2.2. Synthesis of complexes

The complexes were prepared by adding 0.17 g (1.0 mmol) AgNO₃ in 5.0 mL ethanol to 0.15 g (0.5 mmol) *cis*-diamminedi-

chloridoplatinum(II) (cisplatin) in 10 mL ethanol and stirring the mixture for 1 h at 25 °C to precipitate silver chloride. The resultant mixture was filtered to remove silver chloride as a white solid. Then, 1.0 mmol of selenone ligands (1–5) dissolved in 10 mL ethanol or acetonitrile and added, drop-wise, to the filtrates. Stirring the mixture for three h at room temperature resulted in yellow, brown, and grey colored solutions.



- 1) Selenourea (Seu) (Complex 1)
- 2) *N,N'*-dimethylselenourea (Me₂Seu) (Complex 2)
- 3) 1,3-Imidazolidine-2-selenone (ImSe) (Complex 3)
- 4) 1,3-Diazinane-2-selenone (DiazSe) (Complex 4)
- 5) 1,3-Diazepane-2-selenone (DiapSe) (Complex 5)

Fig. 2 Synthesis of *cis*-Pt-selenone compounds from cisplatin.

The solutions were filtered and kept at room temperature for three to five days in an undisturbed area. Solid powder was isolated by slowly evaporating the solvents and kept in the fridge. The synthesis procedure is shown in Fig. 2. The elemental (CHN) analysis data of the complexes are presented in Table 1.

- 1) Selenourea (Seu) (Complex 1)
- 2) N,N'-dimethylselenourea (Me₂Seu) (Complex 2)
- 3) 1,3-Imidazolidine-2-selenone (ImSe) (Complex 3)
- 4) 1,3-Diazinane-2-selenone (DiazSe) (Complex 4)
- 5) 1,3-Diazepane-2-selenone (DiapSe) (Complex 5)

2.3. Instrumentation

Elemental analyses were performed using Perkin Elmer Series 11 (CHNS/O) analyzer 2400. The solid-state FTIR spectra were recorded on a Nicolet 6700 fourier-transform infrared (FTIR) spectrophotometer over the range of 400–4000 cm⁻¹ at a resolution of 4.0 cm⁻¹. Nuclear magnetic resonance (NMR) measurements were carried out in DMSO *d*₆ using a JEOL JNM-LA 500 NMR spectrometer at 297 K. The ¹H and proton-decoupled ¹³C NMR spectra were recorded at 500.00 and 125.65 MHz, respectively. The spectral conditions were: 32 K data points, 0.963 s acquisition time, 2.5 s pulse delay, and 5.12 μs pulse width for ¹H NMR, and 32 K data points, 0.963 s acquisition time, 3.2 s pulse delay, and 5.75 μs pulse width for ¹³C NMR. The chemical shifts were measured relative to tetramethylsilane (TMS). The ⁷⁷Se NMR chemical shifts were recorded at 95.35 MHz relative to an external reference (SeO₂ in D₂O) at 0.00 ppm, using 2.0 s pulse delay and 0.311 s acquisition time.

2.4. Stability studies

Complex 4 as a representative complex was selected for stability studies using Lambda 200, Perkin-Elmer UV-visible spectroscopy. Complex 4 was dissolved in DMSO then subjected to stability examinations at different time points, 0 h, 24 h, and 72 h.

2.5. Computational studies

2.5.1. Quantum chemical calculations

Quantum chemical calculations were performed, in the gas phase, for complexes 1–5 using Gaussian 9 program (Frisch

et al., 2009). Models were built using the Avogadro 1.2.0 program (Hanwell et al., 2012). Fully relaxed ground state geometries for all complexes were obtained at the DFT using the B3LYP DFT, the 6-31 + G(d) basis set for C, H, and N atoms, and the LANL2DZ basis set for Se and Pt atoms. The minimum energy conformation was confirmed using positive vibrational frequencies.

2.5.2. Molecular docking studies

To investigate the mode of interaction of the newly synthesized platinum-selenone complexes, we performed rigid/flexible molecular docking against the DNA duplex (Haleel et al., 2014; Jomaa et al., 2019) with the sequence d (CGCAAATTCGC)₂ dodecamer (PDB ID: 1BNA) (Drew et al., 1981). First, we placed B-DNA in an octahedron bond, added solvent molecules and ions to neutralize the charges, and minimized using the Gromacs 2018 program (Abraham et al., 2015). A further short MD simulation was performed to equilibrate the structure. After MD simulation, the generated DNA structure and the optimized geometries of the Pt-selenone compounds were used for docking. Only the polar hydrogens of the DNA were used for docking. AutoDock Tools (ADT) version 1.5.6 and AutoDock version 4.2.5.1 docking program (Morris et al., 2009) were used for docking the complexes to B-DNA. Gasteiger charges were applied during docking calculations. Molecular docking reportedly plays an important role in the interaction between anti-cancer drugs and DNA molecules (Abou-Dobara et al., 2019; Diab et al., 2019, 2018; El-Sonbati et al., 2020; El-Sonbati et al., 2019; Mohamed et al., 2016; Morgan et al., 2018a, 2018b, 2017; Refaat et al., 2016; Sulaiman et al., 2020a, 2020b). Visualization and analysis of the binding mode and interactions in the binding pocket of the obtained poses were assessed using the VMD program (Humphrey et al., 1996).

2.6. In vitro cytotoxicity of Platinum(II) complexes

Different concentrations (0.5, 1.0, 3.0, 10.0, 30.0, and 100.0 μM) of Pt(II) complexes 1–5 and cisplatin (classical standard control) with concentrations were prepared in Dulbecco's Modified Eagle's Medium (DMEM). A549, HeLa, and HCT116 cells were seeded and maintained in quadruplicate in a 96-well culture plate at 5 × 10⁴ cells/well in 200 μL of the same medium. The cancer cells were incubated for 24 h before treatment. The complexes were dissolved in 50% DMSO stock solutions due to poor aqueous solubility. The

Table 1 Elemental analysis, melting points, color, and yield of *cis*-diammine-platinum(II) complexes of selenones, *cis*-[Pt(NH₃)₂(Selenone)₂](NO₃)₂.

Complex	Found (Calcd) %			M.P.(°C)	Color	Yield %
	C	H	N			
[Pt(NH ₃) ₂ (Seu) ₂](NO ₃) ₂ (1)	3.92 (4.01)	2.40(2.35)	18.87(18.70)	155–158	Brown	77.0%
[Pt(NH ₃) ₂ (Me ₂ Seu) ₂](NO ₃) ₂ (2)	10.88(10.99)	3.46(3.38)	17.27(17.09)	140–144	Gray	80.5%
[Pt(NH ₃) ₂ (ImSe) ₂](NO ₃) ₂ (3)	10.97(11.06)	2.93(2.78)	16.92(17.20)	185–188	Brown	80.0%
[Pt(NH ₃) ₂ (DiazSe) ₂](NO ₃) ₂ (4)	14.55(14.41)	3.39(3.26)	16.27(16.49)	111–115	Brown	78.0%
[Pt(NH ₃) ₂ (DiapSe) ₂](NO ₃) ₂ (5)	16.85(16.97)	3.88(3.70)	15.98(15.84)	188–193	Yellow	81.4%

final DMSO concentration in each treatment group was <0.1%. Therefore, 0.1% DMSO in DMEM was used as a negative control. The cancer cells were treated with the synthesized complexes (1–5) and cisplatin for 24 h. After incubation, the medium from each well was discarded, and 100 μ L DMEM containing 10% 3-(4,5-dimethylthiazol-2-yl)-2,5-diphenyltetrazolium bromide (MTT) dye added to the wells and incubated in the dark for 4 h in a 5% CO₂ incubator at 37 °C. After incubation, a purple-colored formazan (artificial chromogenic dye, a product of the reduction of water-insoluble tetrazolium salts, e.g., MTT by dehydrogenases and reductases) was produced by the cells and appeared as dark crystals at the bottom of the wells. The medium was carefully discarded from each well, making sure to avoid disrupting the monolayer. After this, 100 μ L of isopropanol was added into each well and the solution was mixed thoroughly to dissolve the formazan crystals, resulting in a purple solution. The absorbance of the solution was measured at 570 nm with a Mithras 2LB943 and subtracted from the absorbance of a blank solution. Percentage cell viability was calculated using the formula: Cell viability (%) = 100 \times (absorbance of compound)/(absorbance of control). The IC₅₀ value for each complex was calculated in GraphPad 8.0 and Excel 2016 (Sulaiman et al., 2020a, 2020b).

2.7. Mechanistic studies of complex 3

2.7.1. miRNA expression signatures

The NSCLC cell line, A549, was cultured in 6-well plates at 5×10^5 cells/well for 24 h. The cells were then treated, in duplicate, with either complex 3 at 1.2 μ M IC₅₀ concentration or complex-free medium (negative control) for 24 h. Thereafter, total RNA, including miRNAs, was isolated from each sample using the miRNeasy Mini Kit (Qiagen, Germany). The concentration and quality of RNA samples were measured using a NanoDrop 2000 spectrophotometer (Thermo Fisher Scientific, USA). For miRNA expression profiling, 100 ng of the extracted total RNA was used for RNA labeling and hybridization onto the Agilent Human SurePrint G3 8_60 k v.21 miRNA microarray chip (Agilent Technologies, USA). At the end of the run, raw data files (.Cel) were generated for each sample. The files were uploaded, normalized, and analyzed using GeneSpring GX software (Agilent Technologies, USA). A two-fold-change was set as the cut-off for determining differentially expressed miRNAs in treated versus control samples. Supervised hierarchical clustering analysis was performed based on differentially expressed miRNAs (Alhoshani et al., 2018).

2.7.2. Identification of validated gene targets and enriched pathways

Putative binding sites for the downregulated and upregulated miRNAs at the 3-UTR of all known human mRNAs were screened using the miRWalk 3.0 database (<http://mirwalk.umm.uni-heidelberg.de/>) (Sticht et al., 2018). The only experimentally validated gene targets were selected for further analysis in the miRTarBase database (<http://mirtarbase.cuhk.edu.cn/php/index.php>) (Huang et al., 2019) to reduce false-positive results which miRWalk suffers using.

The validated target genes were used to perform functional enrichment analyses in DAVID Bioinformatics Resources 6.8

(<https://david.ncicrf.gov/>). Kyoto Encyclopedia of Genes and Genomes (KEGG) pathway enrichment analyses were performed. A Fisher exact value and a false discovery rate (FDR) < 0.05 were used as cut-offs to identify significantly enriched pathways (Huang et al., 2007).

2.7.3. PI3K dual activation assay

A549 cells were treated with complex 3 (1.2 μ M) and vehicle (DMSO) for 24 h. PI3K activity was investigated using the Muse™ PI3K Activation Dual Detection Kit. Processed samples were loaded onto Muse cell analyzer (Merck Millipore, Burlington, MA, USA) to determine the expression and phosphorylation status of the PI3K protein. Complex 3-treated samples were expected to have a lower percentage of PI3K-expressing/phosphorylated cell populations.

2.7.4. Annexin V apoptosis assay

A549 cells were treated with either serial concentrations of complex 3 (1 μ M, 5 μ M, 10 μ M, and 30 μ M) or a vehicle (DMSO)-containing medium for 24 h. The apoptotic effect of complex 3 was evaluated using the PE Annexin V Apoptosis Detection Kit with 7-AAD (BioLegend, USA). The kit utilizes two different dyes, Annexin V and 7AAD, to categorize a broad spectrum of apoptotic and non-apoptotic cells. Annexin V binds to phosphatidylserine on the external membrane of apoptotic cells, while 7AAD permeates and stains the DNA of late-stage apoptotic and dead cells. Staining allows the identification of four cell populations: non-apoptotic (viable) cells (Annexin V- /7AAD-), early apoptotic cells (annexin V+ /7AAD-), late apoptotic or dying cells (Annexin V+ /7AAD+), and necrotic (dead) cells (annexin V- /7AAD+). Complex 3 was expected to increase the apoptotic and necrotic cell populations in a dose-dependent manner.

3. Results and discussion

3.1. Synthesis and spectroscopic studies

Cisplatin, *cis*-[Pt(NH₃)₂Cl₂], was first converted into a more reactive nitrate form by the addition of AgNO₃. The selenones were then added at a molar ratio of 1:2 to yield the desired complexes with the composition, [Pt(NH₃)₂(Selenone)₂(NO₃)₂]. The significant IR bands of the selenones and platinum(II) complexes are listed in Table 2. The ν (C = Se) vibration of the selenones around 600–730 cm⁻¹ shifted toward a lower frequency upon complexation. Such IR band shifts are indicative of complex formation as previously reported (Ahmad et al., 2018, 2003, 2002; Alhoshani et al., 2019; Altoum et al., 2017a, 2017b; Isab et al., 2006). The ν (N-H) and ν (C-N) bands were observed at approximately 3200 cm⁻¹ and 1400 cm⁻¹, respectively. The signals near 800 and 1300 cm⁻¹ indicate the presence of nitrate ions (Ahmad et al., 2003; Altoum et al., 2017a; Isab et al., 2002).

The ¹H (N-H protons), ¹³C, and ⁷⁷Se NMR data of the ligands and their complexes in DMSO *d*₆ are listed in Table 3. The ¹³C and ⁷⁷Se NMR spectra of the complexes are presented in (Supplementary Figs. S1-S9). In the ¹H NMR spectra of the complexes, the N-H signal of selenones appeared downfield by approximately 1.0 ppm with respect to its position in free ligands. The deshielding is due to an increase in π , the charac-

Table 2 Selected IR absorptions (cm^{-1}) of selenones and their *cis*-Pt(II) complexes.

Species	$\nu(\text{C} = \text{Se})$	$\nu(\text{NH})$	$\nu(\text{C-N})$	$\nu(\text{NO})_3$
Seu	736	3265	1520	–
1	603	3320, 3222	1410	1349
Me_2Seu	730	3245	1432	–
2	600	3355	1393	1353
ImSe	561	3250	1463	–
3	552	3283	1397	1365
DiazSe	601	3200	1465	–
4	558	3365	1411	1366
DiapSe	615	3224	1453	–
5	600	3299	1324	1396

Table 3 ^1H (for the N-H proton), $^{13}\text{C}\{^1\text{H}\}$, and $^{77}\text{Se}\{^1\text{H}\}$ NMR chemical shifts (ppm) of the *cis*-Pt(II) complexes with selenones in DMSO d_6 .

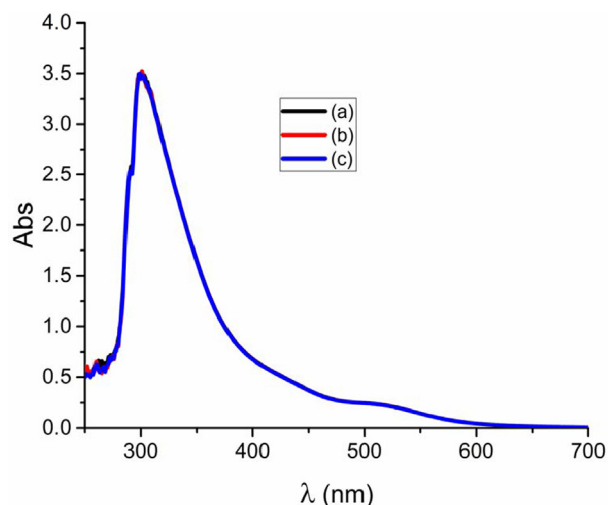
Species	N-H	(C1)C = Se (C1)	N-C2	C3	$\delta(^{77}\text{Se})$
Seu	7.59	178.8	–	–	200.7
1	8.53	168.1	–	–	160.5
Me_2Seu	7.55	177.8	31.0	–	231.4
2	8.39	169.5	31.5	–	185.9
ImSe	8.33	177.1	44.9	–	73.5
3	9.30	166.3	45.7	–	52.3
DiazSe	7.13	171.0	40.8	18.9	199.9
4	7.97	163.5	40.7	18.1	165.5
DiapSe	8.05	180.8	45.5	45.5	292.0
5	8.96	171.0	45.3	45.3	175.9

ter of the C–N bond upon coordination. Selenourea protons were detected at approximately 4 ppm. In the ^{13}C NMR spectra, an upfield shift in the $> \text{C} = \text{Se}$ resonance of selenones was observed upon complexation (Table 3). This upfield shift indicates the coordination of selenone ligands through the selenium atom (Ahmad et al., 2018, 2003, 2002; Alhoshani et al., 2019; Altoum et al., 2017a, 2017b; Isab et al., 2006). The other (C-H) resonances are only slightly shifted.

In the ^{77}Se NMR spectra, the selenone signal shifted upfield upon complexation, providing clear evidence of selenium binding to the metal center. The DiapSe complex, **5**, showed the highest shift difference of 84 ppm, suggesting that it had the highest stability among the prepared complexes. The ^{77}Se shift values are consistent with previously reported data (Alhoshani et al., 2019; Isab et al., 2006; Rani et al., 2017).

3.2. Stability of complex 4

The stability of a representative complex, **4**, was evaluated in DMSO at room temperature using UV-visible spectroscopy. The complex was fully soluble in DMSO. Spectra were taken at 0 h, 24 h, and 72 h as shown in Fig. 3. No changes were observed in the spectra at the three time points. An absorption band was detected at approximately 300 nm, which was associated with the $\pi \rightarrow \pi^*$ transition of the ligands. These observations suggest that complex **4** was stable and did not undergo decomposition in DMSO solution.

**Fig. 3** UV-vis spectra of 0.05 μM complex **4** was performed in DMSO at room temperature. (a) 0 h (b), 24 h (c), 72 h.

3.3. DFT optimized structures

DFT was used to optimize the selenone complexes to obtain the minimum energy conformation. The DFT-optimized

geometries of complexes **1–5** are presented in Fig. 4. In each case, the platinum(II) atom was found to be coordinated by two nitrogen atoms and two selenium atoms, resulting in a square planar geometry. Fig. 4 shows that in the optimized structures, Pt-Se bond length varied between 2.52 Å and 2.54 Å, while the C-Se bond length varied from 1.86 Å in complex **5** to 1.96 Å in complexes **2** and **4**. The shorter bond length

in complex **5** indicates a relatively stronger double bond character of the bond than those in the other complexes (**1–4**). In complexes **1–5**, the C-N bonds have partial double bond characteristics. The bond parameters correspond well with those observed experimentally in other Pt-selenone complexes (Alhoshani et al., 2019; Altoum et al., 2017b; Rani et al., 2017).

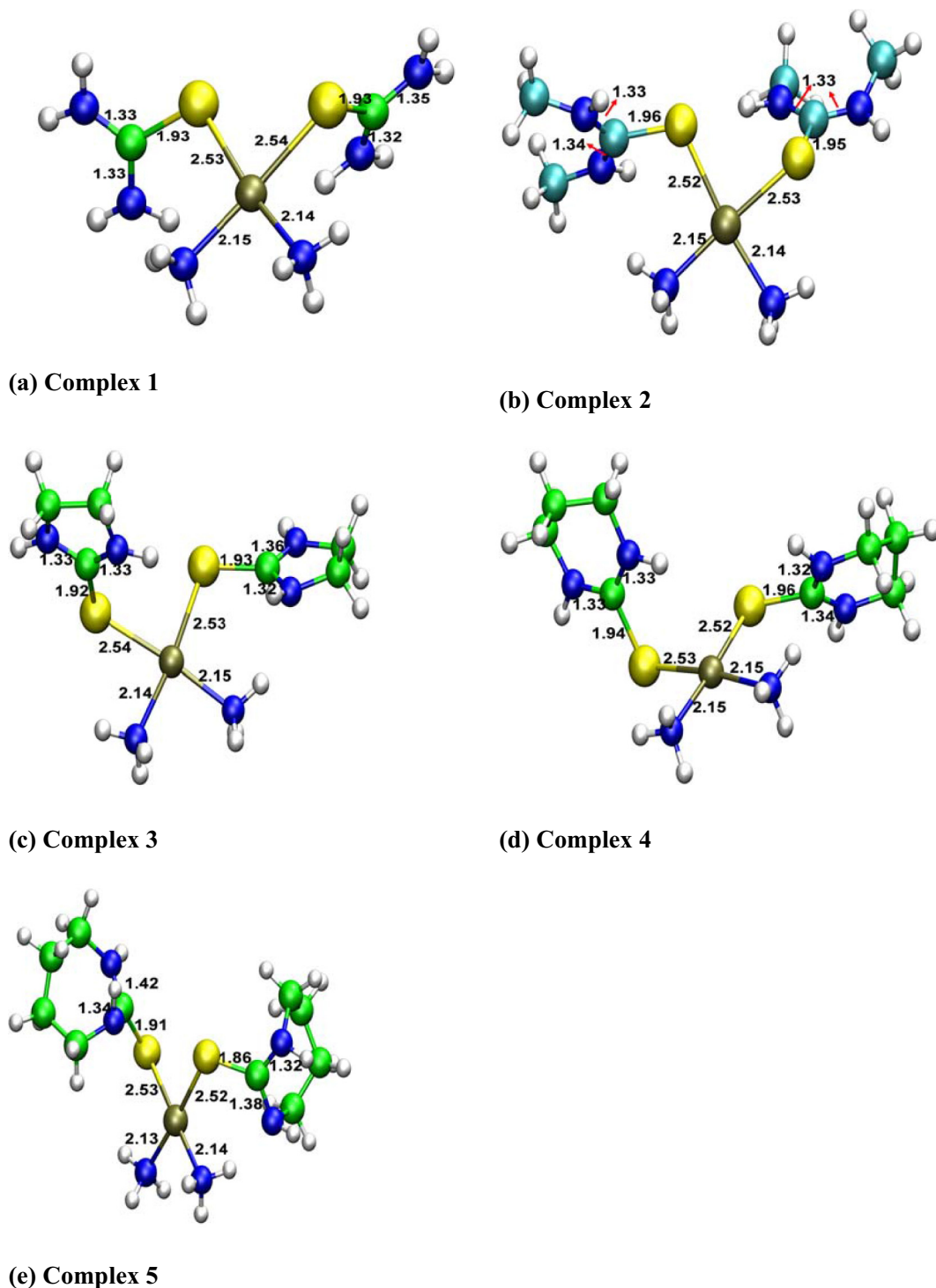


Fig. 4 DFT-optimized structures of Pt-selenone complexes. Bond distances in each complex are shown.

3.4. Molecular docking study

The results of the docking study revealed that the complexes were stabilized primarily by hydrogen bonding interactions with DNA. Table 4 shows the estimated inhibition constants and docking scores for the top-ranked binding conformations. Molecular docking results showed that all studied Pt-selenone complexes bond strongly with the DNA minor groove (Fig. 5 and Supplementary Figs. S10-S14). Binding energy scores were negative for all complexes (1–5). Among the complexes investigated in the study, Complex 5 had the lowest relative binding energy and highest affinity for binding to DNA (Table 4). The best possible conformations of the complexes were obtained via the interactions of their two ammine groups with the base pairs in the minor groove of the DNA, which were stabilized due to stronger hydrogen bonding interactions. All estimated inhibition constants (K_i) for the docking processes were relatively small, implying that the synthesized complexes bind considerably well to the binding sites, and a relatively low concentration of the complexes is sufficient to maximally occupy a binding site and prompt a physiological response.

3.5. In vitro cytotoxicity analyses

In vitro cytotoxicity of complexes (1–5) and cisplatin against three human cancer cells, A549 (lung cancer cells), HeLa (cervical cancer cells), and HCT116 (colon cancer cells), was examined relative to 0.1% DMSO in DMEM using the MTT assay. The impact of treatment with serial concentrations of complexes 1–5 on cancer cell viability and IC_{50} values are illustrated in Fig. 6. complexes, 3 and 4, showed higher *in vitro* cytotoxicity than cisplatin and the other complexes in all three cell lines. Complex 2 exhibited cytotoxicity levels comparable to cisplatin in HCT116 cells, while complex 5 was partially effective against A549 cells only. Complex 1 did not show efficacy against any of the three cell lines tested.

Recently, we reported the anti-cancer properties of other platinum(II) complexes of heterocyclic selenones (Ahmad et al., 2018; Alhoshani et al., 2019; Altoum et al., 2017a, 2017b). Some of these compounds were found to have a better cytotoxic profile than cisplatin (Alhoshani et al., 2019). In our study, complex 3 possessed the highest efficacy among all Pt-selenone complexes that we previously reported (Ahmad et al., 2018; Alhoshani et al., 2019; Altoum et al., 2017a, 2017b). The high sensitivity against cancer cell lines may be ascribed to the presence of ammine groups at the cis position and to their ionic nature (Dasari and Bernard Tchounwou, 2014b), and better accessibility to DNA of cancer cells since

Table 4 Docking results of cisplatin-derived platinum-selenone complexes with the B-DNA (PDB ID: 1BNA).

Complex	Estimated Binding Energy (kcal/mol)	Inhibition Constant (μ M)
1	-7.26	4.80
2	-6.66	13.13
3	-8.12	1.12
4	-8.79	0.36
5	-9.67	0.08

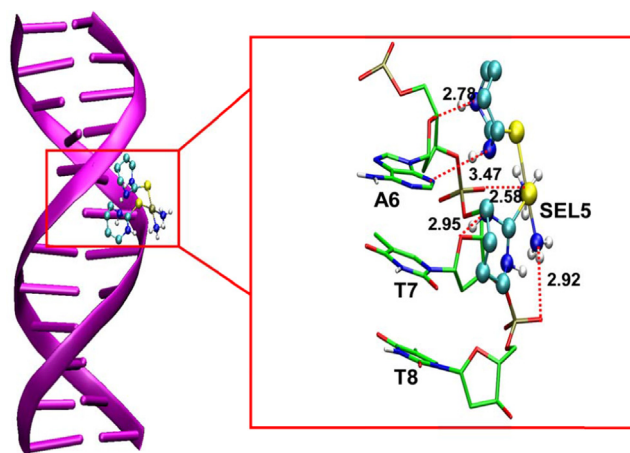


Fig. 5 Analysis of the docking interaction between complex 5 and B-DNA. Hydrogen bonding interactions are shown in the inset.

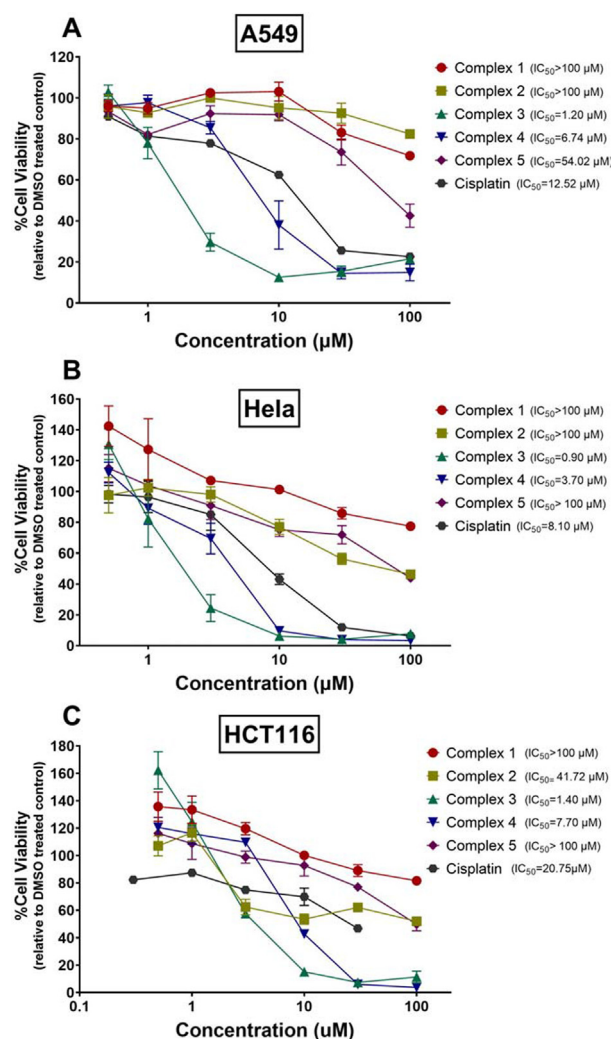


Fig. 6 Effects of different concentrations of *cis*-[Pt(NH₃)₂(-selenone)₂](NO₃)₂ complexes and cisplatin on the viability of cancer cell lines: A) A549 (lung), B) HeLa (cervical), and C) HCT116 (Colon).

complex **3** is a five-membered ring, the smallest among the tested cyclic complexes (Yang and Hinner, 2015).

3.6. Mechanistic studies of complex 3

3.6.1. Impact of complex 3 on miRNA expression signatures in A549

Complex **3** emerged as the most effective candidate in all cancer cell lines tested in this study, including the lung cancer cell line A549 (Fig. 5). Therefore, we investigated the molecular mechanism through which complex **3** exerts its tumor-suppressing effects.

miRNA dysregulation has been demonstrated in many types of cancers, including lung cancer, and has been linked to all cancer hallmarks (Lin et al., 2010; Wu et al., 2019, 2009; Yerukala Sathipati and Ho, 2017). Thus, we performed a microRNA transcriptomic study to understand the impact of complex **3** treatment on miRNA regulation, which ultimately influences the carcinogenic molecular characteristics of the A549 NSCLC cell line, using Human SurePrint miRNA microarray chip technology. We identified 32 out of 866 miRNAs that were differentially expressed with at least a two fold change upon treatment with 1.2 μ M complex **3** relative to the vehicle-treated group. Among these 32 dysregulated miRNAs, 19 were downregulated while 13 were upregulated (Tables 5 and 6). Supervised hierarchical clustering based on the 32 differentially expressed miRNAs clearly separated complex **3**-treated samples from controls (Fig. 7). The data showed that complex **3** altered the A549 miRNA expression profile and this might play an important regulatory role in its cancer-suppressing activity.

3.6.2. Validation of gene targets of differentially expressed miRNAs and pathway enrichment analyses

To understand the role of dysregulated miRNAs in triggering complex **3** anti-cancer activity, we screened for putative bind-

Table 5 Downregulated miRNAs with at least a two-fold change in complex 3-treated samples compared with vehicle-treated controls.

#	miRNA	Fold Change
1	hsa-miR-6815-3p	-53.48
2	hsa-miR-6511a-3p	-44.44
3	hsa-miR-4695-3p	-43.56
4	hsa-miR-3148	-37.79
5	hsa-miR-7152-5p	-25.55
6	hsa-miR-210-5p	-25.21
7	hsa-miR-631	-19.91
8	hsa-miR-6809-3p	-19.45
9	hsa-miR-6760-3p	-19.02
10	hsa-miR-939-3p	-19.00
11	hsa-miR-6803-3p	-18.81
12	hsa-miR-4731-3p	-18.18
13	hsa-miR-6846-3p	-16.86
14	hsa-miR-6819-3p	-16.00
15	hsa-miR-7846-3p	-15.98
16	hsa-miR-149-5p	-15.77
16	hsa-let-7b-3p	-13.26
18	hsa-miR-615-3p	-9.24
19	hsa-miR-1224-3p	-2.39

Table 6 Upregulated miRNAs with at least a two-fold change in complex 3-treated samples compared with vehicle-treated controls.

#	miRNA	Fold Change
1	hsa-miR-4259	78.91
2	hsa-miR-601	43.19
3	hsa-miR-4697-5p	38.98
4	hsa-miR-23a-3p	37.48
5	hsa-miR-130a-3p	33.00
6	hsa-miR-654-5p	31.93
7	hsa-miR-27a-3p	31.90
8	hsa-miR-874-3p	3.28
9	hsa-miR-6126	3.05
10	hsa-miR-5703	2.98
11	hsa-miR-6894-5p	2.79
12	hsa-miR-630	2.61
13	hsa-miR-320c	2.00

ing sites in all known human mRNAs using miRWalk databases and then filtered the predicted gene targets based on literature validation using miRTarBase. We identified 658 validated target genes for the 19 downregulated miRNAs (Supplementary File S1). miR-615-3p had 139 validated target genes, the highest among the downregulated miRNAs (Supplementary Table S1). We identified 370 validated target genes for the 13 upregulated miRNAs (Supplementary File S2). miR-6894-5p had 70 validated target genes, the highest among the upregulated miRNAs (Supplementary Table S2).

We performed pathway enrichment analyses to validate the target genes of differentially expressed miRNAs. No significantly enriched pathway was identified for validated target genes of downregulated miRNAs (Supplementary Table S3) (all had FDR > 0.05). In contrast, six significantly enriched pathways emerged in the analysis of validated target genes of upregulated miRNAs (Table 7). The PI3K/AKT signaling pathway had a 2.27-enrichment fold, with 17 validated target genes, the highest among other significantly enriched pathways. Therefore, we used the PI3K/AKT signaling pathway for further functional validation.

3.6.3. Role of complex 3 in PI3K inhibition

The PI3K/AKT pathway is frequently dysregulated in NSCLC (Balsara, 2004; Cheng et al., 2014; Sarris et al., 2012). Overactivation of the PI3K/AKT pathway plays a role in tumor aggressiveness and therapy resistance (Cully et al., 2006; Fang et al., 2020). Lung adenocarcinoma patients with high *PIK3CA* expression were 1.6 times more likely to die sooner (median survival = 37.17 months) than patients with low expression profiles (median survival = 54.4 months) (Supplementary Fig. S10) (Nagy et al., 2021). Therefore, targeting the PI3K/AKT pathway is a promising approach to reduce oncogenesis and prevent resistance to treatment. We evaluated the impact of complex **3** on PI3K activity using a flow cytometry PI3K dual activation kit. We observed a reduction in PI3K activity in complex **3**-treated cells compared with control cells (Fig. 8A). The cell population that expressed active (phosphorylated) PI3K was suppressed in the complex **3**-treated group (27.6%) compared with the

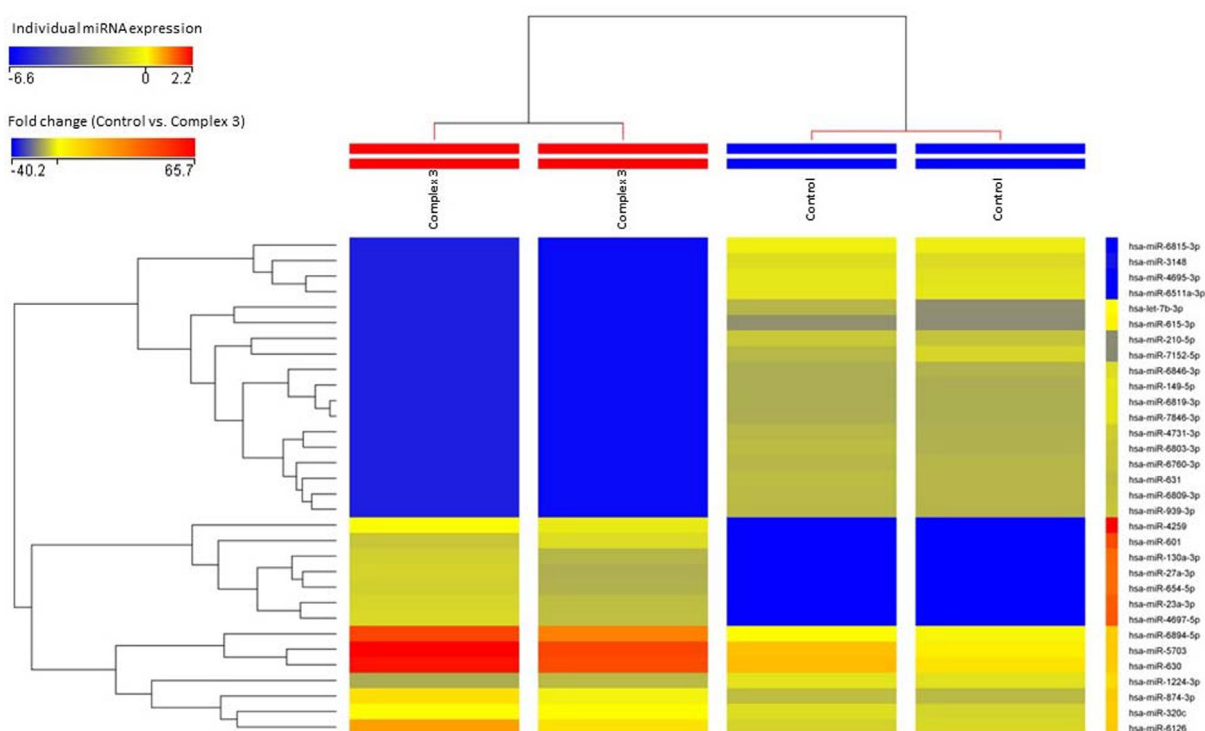


Fig. 7 Supervised hierarchical clustering analysis based on 32 differentially expressed miRNAs following treatment with complex 3.

Table 7 Significantly enriched pathways of upregulated miRNA target genes.

#	Pathway	# Target genes	% Target genes	Fold enrichment	<i>P</i> value*	FDR
1	PI3K-Akt signaling pathway	17	4.70	2.27	0.003	0.035
2	MAPK signaling pathway	15	4.14	2.74	0.001	0.021
3	FoxO signaling pathway	13	3.59	4.48	< 0.001	0.003
4	p53 signaling pathway	10	2.76	6.89	< 0.001	0.002
5	Cell cycle	10	2.76	3.72	0.001	0.022
6	Prolactin signaling pathway	8	2.21	5.20	0.001	0.020

* *P* values based on Fisher's exact test. FDR = False discovery rate.

vehicle-treated group (39.91%). On the contrary, the inactive (unphosphorylated) PI3K was elevated in the complex 3-treated group (49.2%) compared with the vehicle-treated group (25.8%) (Fig. 8B). These results collectively suggest that complex 3 deactivates PI3K in A549 cells and this might be an underlying molecular mechanism contributing to the anti-cancer activity this complex. Deactivation of PI3K might be attributed to: a direct inhibition on the protein level or activity, the upregulation of miR-23a-3p which has been found to target *PIK3R1*, which encodes the regulatory subunit of PI3K (Huang et al., 2019), or a cooperative inhibitory role of the upregulated miRNAs on the pathway as a whole. Future in-depth pharmacological studies are warranted to investigate these scenarios.

3.6.4. Effect of complex 3 on apoptosis

We examined the effect of complex 3 on apoptosis using an Annexin V-PE/7ADD based flow cytometry assay. Treatment

of A549 cells with complex 3 for 24 h induced significant apoptosis in a dose-dependent manner (Fig. 8C). The total percentages of apoptotic cell population increased from 6.7% in the control group (0.1% DMSO) to 18.2%, 47.1%, 71.7%, and 87.8% in the groups that were treated with 1 μ M, 5 μ M, 10 μ M, 30 μ M of complex 3, respectively (Fig. 8D). These results support the hypothesis that induction of apoptosis is an essential molecular mechanism through which complex 3 mediates cytotoxic activity in A549 cells.

4. Conclusion

Five new platinum(II)-selenone complexes derived from cisplatin were synthesized and characterized by elemental analysis, IR, and NMR (^1H , ^{13}C , and ^{77}Se) spectroscopy. The gas phase structures of the complexes were analyzed using DFT calculations. Docking studies showed a favorable interaction with the DNA structure, and the *cis*-[Pt(NH₃)₂(selenone)₂]²⁺

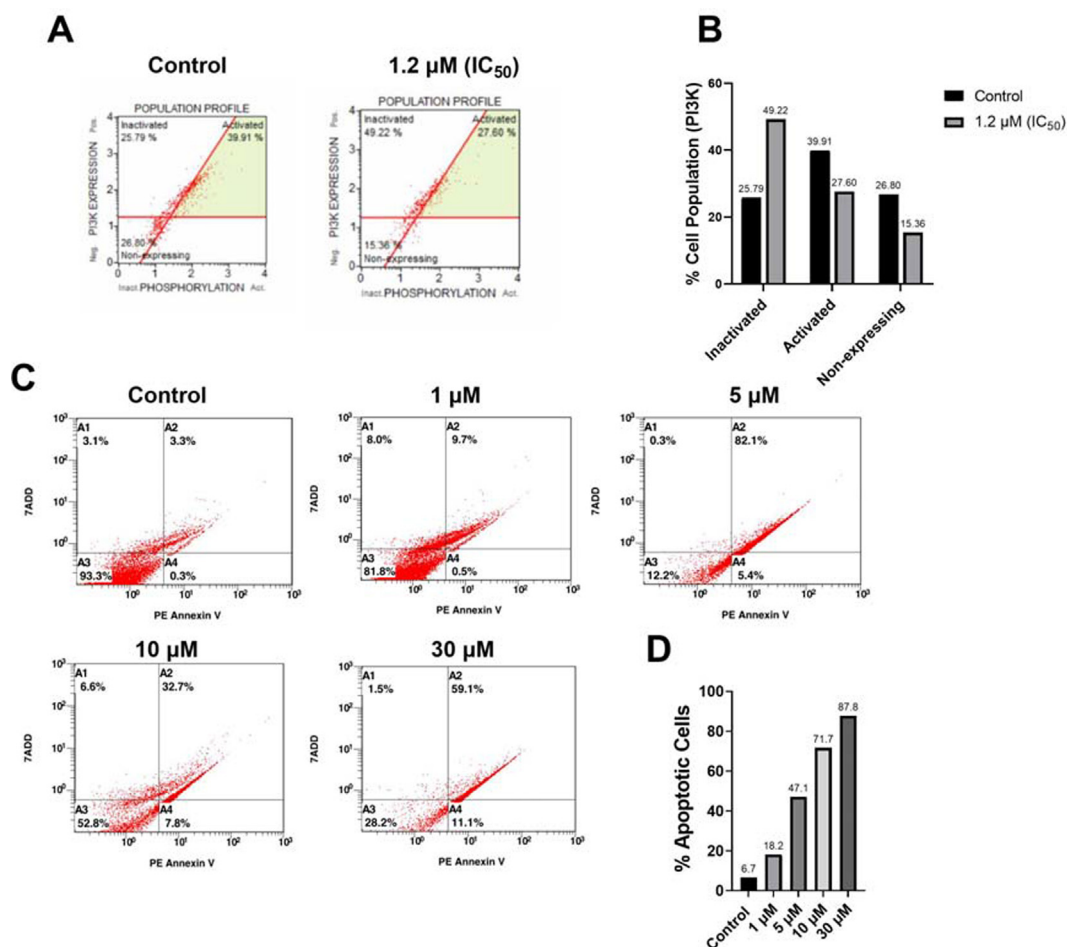


Fig. 8 Influence of complex 3 on PI3K deactivation and apoptosis induction in A549 cells. A) Flow cytometry figures illustrating PI3K expression and activity in control and complex 3-treated samples. B) Percentages of cell populations in the three investigated PI3K statuses: inactivated, activated, and non-expressing cells in control and complex 3 treated samples. C) Flow cytometry figures showing the apoptosis status in control, 1 μM, 5 μM, 10 μM, 30 μM complex 3-treated groups. D) Total percentage of apoptotic cell populations in the treated groups.

species bound to the minor groove of the DNA. The examination of *in vitro* anti-cancer activity against a number of human cancer cell lines (HeLa, A549, and HCT116) revealed that, among the complexes that tested, complex 3 had the highest efficacy and modulated the miRNA expression profile of A549 cells. The PI3K/AKT signaling pathway emerged as a promising target in the pathway enrichment analyses of differentially expressed miRNA gene targets. These results were validated experimentally and showed, compared with control A549 cells, complex 3 deactivated PI3K protein and induced apoptosis. We believe that our work provides new potential therapeutics for the treatment of lung cancer. However, additional *in vivo* and *in vitro* testing of complex 3 are needed to examine toxicity on normal tissues and confirm anti-cancer effects.

Declaration of Competing Interest

The authors declare that they have no known competing financial interests or personal relationships that could have appeared to influence the work reported in this paper.

Acknowledgment

The authors greatly appreciate and thank the financial support provided by King Fahd University of Petroleum and Minerals under project No. **SB181009**.

Appendix A. Supplementary data

Supplementary data to this article can be found online at <https://doi.org/10.1016/j.arabjc.2021.103245>.

References

- Abou-Dobara, M.I., Omar, N.F., Diab, M.A., El-Sonbati, A.Z., Morgan, S.M., El-Mogazy, M.A., 2019. Allyl rhodanine azo dye derivatives: Potential antimicrobials target *scp* - alanyl carrier protein ligase and nucleoside diphosphate kinase. *J. Cell. Biochem.* 120. <https://doi.org/10.1002/jcb.27473>.
- Abraham, M.J., Murtola, T., Schulz, R., Páll, S., Smith, J.C., Hess, B., Lindahl, E., 2015. GROMACS: High performance molecular simulations through multi-level parallelism from laptops to

- supercomputers. *SoftwareX* 1–2. <https://doi.org/10.1016/j.softx.2015.06.001>.
- Ahmad, S., 2017. Kinetic aspects of platinum anticancer agents. *Polyhedron* 138, 109–124. <https://doi.org/10.1016/j.poly.2017.09.016>.
- Ahmad, S., Altom, A.O.S., Vančo, J., Křikavová, R., Trávníček, Z., Dvořák, Z., Altaf, M., Sohail, M., Isab, A.A., 2018. Synthesis, crystal structure and anticancer activity of tetrakis(N-isopropylimidazolidine-2-selenone)platinum(II) chloride. *J. Mol. Struct.* 1152. <https://doi.org/10.1016/j.molstruc.2017.09.068>.
- Ahmad, S., Isab, A.A., Al-Arfaj, A.R., Arnold, A.P., 2002. Synthesis of cyano(selenone)gold(I) complexes and investigation of their scrambling reactions using ¹³C and ¹⁵N NMR spectroscopy. *Polyhedron* 21. [https://doi.org/10.1016/S0277-5387\(02\)01152-X](https://doi.org/10.1016/S0277-5387(02)01152-X).
- Ahmad, S., Isab, A.A., Arnold, A.P., 2003. Synthesis and Spectroscopic Characterization of Silver(I) Complexes of Selenones. *J. Coord. Chem.* 56. <https://doi.org/10.1080/0095897031000101457>.
- Alhoshani, A., Alrashdi, A., Alhosaini, K., Alanazi, F.E., Alajez, N. M., Altaf, M., Isab, A.A., Korashy, H.M., 2018. Gold-containing compound BDG-I inhibits the growth of A549 lung cancer cells through the deregulation of miRNA expression. *Saudi Pharm. J.* 26, 1035–1043. <https://doi.org/10.1016/j.jsps.2018.05.012>.
- Alhoshani, A., Seliman, A.A.A., Altom, A.O., Abuelizz, H.A., Ahmad, S., Altaf, M., Omer, K.H., Sohail, M., Isab, A.A., 2019. Synthesis, X-ray structure and *in vitro* cytotoxicity of transdiammineplatinum(II) complexes of selenones, trans-[Pt(NH₃)₂(selenone)₂](NO₃)₂. *Polyhedron* 158. <https://doi.org/10.1016/j.poly.2018.09.010>.
- Altom, A.O.S., Alhoshani, A., Alhosaini, K., Altaf, M., Ahmad, S., Popoola, S.A., Al-Saadi, A.A., Sulaiman, A.A., Isab, A.A., 2017a. Synthesis, characterization and *in vitro* cytotoxicity of platinum(II) complexes of selenones [Pt(selenone)₂Cl₂]. *J. Coord. Chem.* 70. <https://doi.org/10.1080/00958972.2017.1287355>.
- Altom, A.O.S., Vančo, J., Křikavová, R., Trávníček, Z., Dvořák, Z., Altaf, M., Ahmad, S., Sulaiman, A.A.A., Isab, A.A., 2017b. Synthesis, structural characterization and cytotoxicity evaluation of platinum(II) complexes of heterocyclic selenones. *Polyhedron* 128. <https://doi.org/10.1016/j.poly.2017.02.027>.
- American Cancer Society, 2021. *Cancer Facts & Figures 2021*.
- Bai, L., Gao, C., Liu, Q., Yu, C., Zhang, Z., Cai, L., Yang, B., Qian, Y., Yang, J., Liao, X., 2017. Research progress in modern structure of platinum complexes. *Eur. J. Med. Chem.* 140. <https://doi.org/10.1016/j.ejmech.2017.09.034>.
- Balsara, B.R., 2004. Frequent activation of AKT in non-small cell lung carcinomas and preneoplastic bronchial lesions. *Carcinogenesis* 25, 2053–2059. <https://doi.org/10.1093/carcin/bgh226>.
- Bartel, D.P., 2004. MicroRNAs: Genomics, Biogenesis, Mechanism, and Function. *Cell* 116, 281–297. [https://doi.org/10.1016/S0092-8674\(04\)00045-5](https://doi.org/10.1016/S0092-8674(04)00045-5).
- Bernhardt, G., Brunner, H., Gruber, N., Lottner, C., Pushpan, S.K., Tsuno, T., Zabel, M., 2004. Carboplatin derivatives with superior antitumor activity compared to the parent compound. *Inorg. Chim. Acta* 357. <https://doi.org/10.1016/j.ica.2004.03.060>.
- Carland, M., Abrahams, B.F., Rede, T., Stephenson, J., Murray, V., Denny, W.A., McFadyen, W.D., 2006. Syntheses and structural studies of platinum(II) complexes of O-methylselenomethionine and related ligands. *Inorg. Chim. Acta* 359. <https://doi.org/10.1016/j.ica.2006.03.008>.
- Catalanotto, C., Cogoni, C., Zardo, G., 2016. MicroRNA in Control of Gene Expression: An Overview of Nuclear Functions. *Int. J. Mol. Sci.* 17. <https://doi.org/10.3390/ijms17101712>.
- Cheng, H., Shcherba, M., Pendurti, G., Liang, Y., Piperdi, B., Perez-Soler, R., 2014. Targeting the PI3K/AKT/mTOR pathway: potential for lung cancer treatment. *Lung Cancer Manage.* 3, 67–75. <https://doi.org/10.2217/lmt.13.72>.
- Chopade, S.M., Phadnis, P.P., Hodage, A.S., Wadawale, A., Jain, V. K., 2015. Synthesis, characterization, structures and cytotoxicity of platinum(II) complexes containing dimethylpyrazole based selenonium ligands. *Inorg. Chim. Acta* 427. <https://doi.org/10.1016/j.ica.2014.11.017>.
- Cristiani, F., Devillanova, F.A., Verani, G., 1977. Infrared study of 1,3-thiazolidin(e)-2-one, -2-thione, and -2-selone and their 1-oxa-analogues. *J. Chem. Soc., Perkin Trans. 2*, 324–327. <https://doi.org/10.1039/p29770000324>.
- Cully, M., You, H., Levine, A.J., Mak, T.W., 2006. Beyond PTEN mutations: the PI3K pathway as an integrator of multiple inputs during tumorigenesis. *Nat. Rev. Cancer* 6, 184–192. <https://doi.org/10.1038/nrc1819>.
- Dasari, S., Bernard Tchounwou, P., 2014a. Cisplatin in cancer therapy: Molecular mechanisms of action. *Eur. J. Pharmacol.* 740, 364–378. <https://doi.org/10.1016/j.ejphar.2014.07.025>.
- Dasari, S., Bernard Tchounwou, P., 2014b. Cisplatin in cancer therapy: Molecular mechanisms of action. *Eur. J. Pharmacol.* 740. <https://doi.org/10.1016/j.ejphar.2014.07.025>.
- Deo, K.M., Ang, D.L., McGhie, B., Rajamanickam, A., Dhiman, A., Khoury, A., Holland, J., Bjelosevic, A., Pages, B., Gordon, C., Aldrich-Wright, J.R., 2018. Platinum coordination compounds with potent anticancer activity. *Coord. Chem. Rev.* 375. <https://doi.org/10.1016/j.ccr.2017.11.014>.
- Diab, M.A., El-Sonbati, A.Z., Morgan, Sh.M., El-Mogazy, M.A., 2018. Polymer complexes. LXXI. Spectroscopic studies, thermal properties, DNA binding and antimicrobial activity of polymer complexes. *Appl. Organomet. Chem.* 32. <https://doi.org/10.1002/aoc.4378>.
- Diab, M.A., Mohamed, G.G., Mahmoud, W.H., El-Sonbati, A.Z., Morgan, Sh.M., Abbas, S.Y., 2019. Inner metal complexes of tetradentate Schiff base: Synthesis, characterization, biological activity and molecular docking studies. *Appl. Organomet. Chem.* 33. <https://doi.org/10.1002/aoc.4945>.
- Dilruba, S., Kalayda, G.V., 2016. Platinum-based drugs: past, present and future. *Cancer Chemother. Pharmacol.* 77, 1103–1124. <https://doi.org/10.1007/s00280-016-2976-z>.
- Drew, H.R., Wing, R.M., Takano, T., Broka, C., Tanaka, S., Itakura, K., Dickerson, R.E., 1981. Structure of a B-DNA Dodecamer: Conformation and Dynamics. *PNAS* 78, 2179–2183.
- El-Sonbati, A.Z., Diab, M.A., Eldesoky, A.M., Morgan, S.M., Salem, O.L., 2019. Polymer complexes. LXXVI. Synthesis, characterization, CT-DNA binding, molecular docking and thermal studies of sulfoxine polymer complexes. *Appl. Organomet. Chem.* 33. <https://doi.org/10.1002/aoc.4839>.
- El-Sonbati, A.Z., Diab, M.A., Morgan, Sh.M., Abou-Dobara, M.I., El-Ghettany, A.A., 2020. Synthesis, characterization, theoretical and molecular docking studies of mixed-ligand complexes of Cu (II), Ni(II), Co(II), Mn(II), Cr(III), UO₂(II) and Cd(II). *J. Mol. Struct.* 1200. <https://doi.org/10.1016/j.molstruc.2019.127065>.
- Escribano, E., Font-Bardia, M., Calvet, T., Lorenzo, J., Gamez, P., Moreno, V., 2013. DNA binding studies of a series of cis-[Pt(Am)₂X₂] complexes (Am = inert amine, X = labile carboxylato ligand). *Inorg. Chim. Acta* 394. <https://doi.org/10.1016/j.ica.2012.07.018>.
- Fang, W., Huang, Yihua, Gu, W., Gan, J., Wang, W., Zhang, S., Wang, K., Zhan, J., Yang, Y., Huang, Yan, Zhao, H., Zhang, L., 2020. PI3K-AKT-mTOR pathway alterations in advanced NSCLC patients after progression on EGFR-TKI and clinical response to EGFR-TKI plus everolimus combination therapy. *Translational Lung Cancer Res.* 9, 1258–1267. <https://doi.org/10.21037/tlcr-20-141>.
- Fennell, D.A., Summers, Y., Cadranel, J., Benepal, T., Christoph, D. C., Lal, R., Das, M., Maxwell, F., Visseren-Grul, C., Ferry, D., 2016. Cisplatin in the modern era: The backbone of first-line chemotherapy for non-small cell lung cancer. *Cancer Treat. Rev.* 44, 42–50. <https://doi.org/10.1016/j.ctrv.2016.01.003>.
- Florea, A.-M., Büsselberg, D., 2011. Cisplatin as an Anti-Tumor Drug: Cellular Mechanisms of Activity, Drug Resistance and Induced Side Effects. *Cancers* 3, 1351–1371. <https://doi.org/10.3390/cancers3011351>.

- Frisch, M.J., Trucks, G.W., Schlegel, H.B., Scuseria, G.E., Robb, M. A., Cheeseman, J.R., Scalmani, G., Barone, V., Petersson, G.A., Nakatsuji, H., Li, X., Caricato, M., Marenich, A., Bloino, J., Janesko, B.G., Gomperts, R., Mennucci, B., Hratchian, H.P., Ortiz, J. V., Izmaylov, A.F., et al., 2009. Gaussian 09.
- Fuks, L., Anuszcwska, E., Kruszcwska, H., Króczyński, A., Dudek, J., Sadlej-Sosnowska, N., 2010. Platinum(II) complexes with thiourea derivatives containing oxygen, sulfur or selenium in a heterocyclic ring: computational studies and cytotoxic properties. *Transition Met. Chem.* 35. <https://doi.org/10.1007/s11243-010-9375-9>.
- Galanski, M., Jakupec, M., Keppler, B., 2005. Update of the Preclinical Situation of Anticancer Platinum Complexes: Novel Design Strategies and Innovative Analytical Approaches. *Curr. Med. Chem.* 12, 2075–2094. <https://doi.org/10.2174/0929867054637626>.
- Galluzzi, L., Senovilla, L., Vitale, I., Michels, J., Martins, I., Kepp, O., Castedo, M., Kroemer, G., 2012. Molecular mechanisms of cisplatin resistance. *Oncogene* 31, 1869–1883. <https://doi.org/10.1038/onc.2011.384>.
- Gay, M., Montaña, Á.M., Batalla, C., Mesas, J.M., Alegre, M.-T., 2015. Design, synthesis and SAR studies of novel 1,2-bis(aminomethyl)cyclohexane platinum(II) complexes with cytotoxic activity. Studies of interaction with DNA of iodinated seven-membered 1,4-diaminoplatinocycles. *J. Inorg. Biochem.* 142. <https://doi.org/10.1016/j.jinorgbio.2014.09.012>.
- Haleel, A., Arthi, P., Dastagiri Reddy, N., Veena, V., Sakthivel, N., Arun, Y., Perumal, P.T., Kalilur Rahiman, A., 2014. DNA binding, molecular docking and apoptotic inducing activity of nickel(<sc>ii</sc>), copper(<sc>ii</sc>) and zinc (<sc>ii</sc>) complexes of pyridine-based tetrazolo[1,5-a]pyrimidine ligands. *RSC Adv.* 4. <https://doi.org/10.1039/C4RA11197D>.
- Hanwell, M.D., Curtis, D.E., Lonie, D.C., Vandermeersch, T., Zurek, E., Hutchison, G.R., 2012. Avogadro: an advanced semantic chemical editor, visualization, and analysis platform. *J. Cheminf.* 4. <https://doi.org/10.1186/1758-2946-4-17>.
- Ho, G.Y., Woodward, N., Coward, J.I.G., 2016. Cisplatin versus carboplatin: comparative review of therapeutic management in solid malignancies. *Crit. Rev. Oncol./Hematol.* 102, 37–46. <https://doi.org/10.1016/j.critrevonc.2016.03.014>.
- Huang, D., Sherman, B.T., Tan, Q., Collins, J.R., Alvord, W.G., Roayaei, J., Stephens, R., Baseler, M.W., Lane, H.C., Lempicki, R. A., 2007. The DAVID Gene Functional Classification Tool: a novel biological module-centric algorithm to functionally analyze large gene lists. *Genome Biol.* 8, R183. <https://doi.org/10.1186/gb-2007-8-9-r183>.
- Huang, H.-Y., Lin, Y.-C.-D., Li, J., Huang, K.-Y., Shrestha, S., Hong, H.-C., Tang, Y., Chen, Y.-G., Jin, C.-N., Yu, Y., Xu, J.-T., Li, Y.-M., Cai, X.-X., Zhou, Z.-Y., Chen, X.-H., Pei, Y.-Y., Hu, L., Su, J.-J., Cui, S.-D., Wang, F., Xie, Y.-Y., Ding, S.-Y., Luo, M.-F., Chou, C.-H., Chang, N.-W., Chen, K.-W., Cheng, Y.-H., Wan, X.-H., Hsu, W.-L., Lee, T.-Y., Wei, F.-X., Huang, H.-D., 2019. miRTarBase 2020: updates to the experimentally validated microRNA–target interaction database. *Nucleic Acids Res.* <https://doi.org/10.1093/nar/gkz896>.
- Humphrey, W., Dalke, A., Schulten, K., 1996. VMD: Visual molecular dynamics. *J. Mol. Graph.* 14. [https://doi.org/10.1016/0263-7855\(96\)00018-5](https://doi.org/10.1016/0263-7855(96)00018-5).
- Intini, F.P., Zajac, J., Novohradsky, V., Saltarella, T., Pacifico, C., Brabec, V., Natile, G., Kasparkova, J., 2017. Novel Antitumor Platinum(II) Conjugates Containing the Nonsteroidal Anti-inflammatory Agent Diclofenac: Synthesis and Dual Mechanisms of Antiproliferative Effects. *Inorg. Chem.* 56. <https://doi.org/10.1021/acs.inorgchem.6b02553>.
- Isab, A.A., Ahmad, S., Arab, M., 2002. Synthesis of silver(I) complexes of thiones and their characterization by ¹³C, ¹⁵N and ¹⁰⁷Ag NMR spectroscopy. *Polyhedron* 21. [https://doi.org/10.1016/S0277-5387\(02\)00981-6](https://doi.org/10.1016/S0277-5387(02)00981-6).
- Isab, A.A., Wazeer, M.I.M., Fettouhi, M., Ahmad, S., Ashraf, W., 2006. Synthesis and characterization of mercury(II) complexes of selones: X-ray structures, CP MAS and solution NMR studies. *Polyhedron* 25. <https://doi.org/10.1016/j.poly.2006.03.022>.
- Jansson, M.D., Lund, A.H., 2012. MicroRNA and cancer. *Mol. Oncol.* 6, 590–610. <https://doi.org/10.1016/j.molonc.2012.09.006>.
- Johnstone, T.C., Suntharalingam, K., Lippard, S.J., 2016. The Next Generation of Platinum Drugs: Targeted Pt(II) Agents, Nanoparticle Delivery, and Pt(IV) Prodrugs. *Chem. Rev.* 116, 3436–3486. <https://doi.org/10.1021/acs.chemrev.5b00597>.
- Jomaa, M.Y., Ahmad, S., Seliman, A.A.A., Popoola, S.A., Shaikh, A.R., Al-Saadi, A.A., Bhatia, G., Singh, J., Isab, A.A., 2019. Synthesis, spectroscopic characterization and *in vitro* cytotoxic as well as docking studies of cis-diammine platinum(II) complexes of thiones. *Inorg. Chim. Acta* 484. <https://doi.org/10.1016/j.ica.2018.09.070>.
- Jonas, S., Izaurralde, E., 2015. Towards a molecular understanding of microRNA-mediated gene silencing. *Nat. Rev. Genet.* 16, 421–433. <https://doi.org/10.1038/nrg3965>.
- Kelland, L., 2007. The resurgence of platinum-based cancer chemotherapy. *Nat. Rev. Cancer* 7, 573–584. <https://doi.org/10.1038/nrc2167>.
- Kelland, L.R., Sharp, S.Y., O'Neill, C.F., Raynaud, F.I., Beale, P.J., Judson, I.R., 1999. Mini-review: discovery and development of platinum complexes designed to circumvent cisplatin resistance. *J. Inorg. Biochem.* 77, 111–115.
- Kovala-Demertzi, D., Papageorgiou, A., Papathanasis, L., Alexandratos, A., Dalezis, P., Miller, J.R., Demertzis, M.A., 2009. *In vitro* and *in vivo* antitumor activity of platinum(II) complexes with thiosemicarbazones derived from 2-formyl and 2-acetyl pyridine and containing ring incorporated at N(4)-position: Synthesis, spectroscopic study and crystal structure of platinum(II) complexes with thiosemicarbazones, potential anticancer agents. *Eur. J. Med. Chem.* 44. <https://doi.org/10.1016/j.ejmech.2008.08.007>.
- Křikavová, R., Vančo, J., Šilha, T., Marek, J., Trávníček, Z., 2016. Synthesis, characterization, DNA binding studies and *in vitro* cytotoxicity of platinum(II)-dihalogenido complexes containing bidentate chelating N - donor ligands. *J. Coord. Chem.* 69. <https://doi.org/10.1080/00958972.2016.1199862>.
- Kurozumi, S., Yamaguchi, Y., Kurozumi, M., Ohira, M., Matsumoto, H., Horiguchi, J., 2016. Recent trends in microRNA research into breast cancer with particular focus on the associations between microRNAs and intrinsic subtypes. *J. Hum. Genet.* 62, 15.
- Lebwohl, D., Canetta, R., 1998. Clinical development of platinum complexes in cancer therapy: an historical perspective and an update. *Eur. J. Cancer* 34, 1522–1534. [https://doi.org/10.1016/S0959-8049\(98\)00224-X](https://doi.org/10.1016/S0959-8049(98)00224-X).
- Lin, P.-Y., Yu, S.-L., Yang, P.-C., 2010. MicroRNA in lung cancer. *Br. J. Cancer* 103, 1144–1148. <https://doi.org/10.1038/sj.bjc.6605901>.
- Lovejoy, K.S., Lippard, S.J., 2009. Non-traditional platinum compounds for improved accumulation, oral bioavailability, and tumor targeting. *Dalton Trans.* 10651. <https://doi.org/10.1039/b913896j>.
- Marverti, G., Cusumano, M., Ligabue, A., Di Pietro, M.L., Vainiglia, P.A., Ferrari, A., Bergomi, M., Moruzzi, M.S., Frassinetti, C., 2008. Studies on the anti-proliferative effects of novel DNA-intercalating bipyridyl–thiourea–Pt(II) complexes against cisplatin-sensitive and -resistant human ovarian cancer cells. *J. Inorg. Biochem.* 102. <https://doi.org/10.1016/j.jinorgbio.2007.10.015>.
- Miles, B.A., Patterson, A.E., Vogels, C.M., Decken, A., Waller, J.C., Morin Jr., P., Westcott, S.A., 2016. Synthesis, characterization, and anticancer activities of lipophilic pyridinecarboxaldehyde platinum (II) complexes. *Polyhedron* 108. <https://doi.org/10.1016/j.poly.2015.07.039>.

- Mohamed, G.G., El-Sherif, A.A., Saad, M.A., El-Sawy, S.E.A., Morgan, Sh.M., 2016. Mixed-ligand complex formation of tenoxicam drug with some transition metal ions in presence of valine: Synthesis, characterization, molecular docking, potentiometric and evaluation of the humeral immune response of calves. *J. Mol. Liq.* 223. <https://doi.org/10.1016/j.molliq.2016.09.065>.
- Morgan, Sh.M., Diab, M.A., El-Sonbati, A.Z., 2018a. Synthesis, molecular geometry, spectroscopic studies and thermal properties of Co(II) complexes. *Appl. Organomet. Chem.* 32. <https://doi.org/10.1002/aoc.4305>.
- Morgan, Sh.M., Diab, M.A., El-Sonbati, A.Z., 2018b. Supramolecular assembly of hydrogen bonding, ESR studies and theoretical calculations of Cu(II) complexes. *Appl. Organomet. Chem.* 32. <https://doi.org/10.1002/aoc.4504>.
- Morgan, Sh.M., El-Sonbati, A.Z., Eissa, H.R., 2017. Geometrical structures, thermal properties and spectroscopic studies of Schiff base complexes: Correlation between ionic radius of metal complexes and DNA binding. *J. Mol. Liq.* 240. <https://doi.org/10.1016/j.molliq.2017.05.114>.
- Morris, G.M., Huey, R., Lindstrom, W., Sanner, M.F., Belew, R.K., Goodsell, D.S., Olson, A.J., 2009. AutoDock4 and AutoDockTools4: Automated docking with selective receptor flexibility. *J. Comput. Chem.* 30. <https://doi.org/10.1002/jcc.21256>.
- Nagy, Á., Munkácsy, G., Gyórfy, B., 2021. Pancancer survival analysis of cancer hallmark genes. *Sci. Rep.* 11, 6047. <https://doi.org/10.1038/s41598-021-84787-5>.
- Noone, A., Howlader, N., Krapcho, M., Miller, D., Brest, A., Yu, M., Ruhl, J., Tatalovich, Z., Mariotto, A., Lewis, D., Chen, H., Feuer, E., Cronin, K., 2018. SEER Cancer Statistics Review, 1975–2015. National Cancer Institute, Bethesda, MD.
- Oun, R., Moussa, Y.E., Wheate, N.J., 2018. The side effects of platinum-based chemotherapy drugs: a review for chemists. *Dalton Trans.* 47, 6645–6653. <https://doi.org/10.1039/C8DT00838H>.
- Peng, Y., Croce, C.M., 2016. The role of MicroRNAs in human cancer. *Signal Transd. Targeted Therapy* 1, 15004.
- Piccolini, V.M., Bottone, M.G., Bottioli, G., De Pascali, S.A., Fanizzi, F.P., Bernocchi, G., 2013. Platinum drugs and neurotoxicity: effects on intracellular calcium homeostasis. *Cell Biol. Toxicol.* 29, 339–353. <https://doi.org/10.1007/s10565-013-9252-3>.
- Pracharova, J., Saltarella, T., Radosova Muchova, T., Scintilla, S., Novohradsky, V., Novakova, O., Intini, F.P., Pacifico, C., Natile, G., Ilik, P., Brabec, V., Kasparkova, J., 2015. Novel Antitumor Cisplatin and Transplatin Derivatives Containing 1-Methyl-7-Azaindole: Synthesis, Characterization, and Cellular Responses. *J. Med. Chem.* 58. <https://doi.org/10.1021/jm501420k>.
- Rani, V., Singh, H.B., Butcher, R.J., 2017. Bis(selone) Complexes of Palladium(II), Platinum(II), and Gold(III): Synthesis and Structural Studies. *Eur. J. Inorg. Chem.* 2017. <https://doi.org/10.1002/ejic.201700377>.
- Reedijk, J., 2009. Platinum Anticancer Coordination Compounds: Study of DNA Binding Inspires New Drug Design. *Eur. J. Inorg. Chem.* 2009, 1303–1312. <https://doi.org/10.1002/ejic.200900054>.
- Refaat, H.M., El-Badway, H.A., Morgan, Sh.M., 2016. Molecular docking, geometrical structure, potentiometric and thermodynamic studies of moxifloxacin and its metal complexes. *J. Mol. Liq.* 220. <https://doi.org/10.1016/j.molliq.2016.04.124>.
- Sarris, E., Saif, M., Syrigos, K., 2012. The Biological Role of PI3K Pathway in Lung Cancer. *Pharmaceuticals* 5, 1236–1264. <https://doi.org/10.3390/ph5111236>.
- Schirle, N.T., Sheu-Gruttadauria, J., MacRae, I.J., 2014. Structural basis for microRNA targeting. *Science* 346. <https://doi.org/10.1126/science.1258040>.
- Shen, D.-W., Pouliot, L.M., Hall, M.D., Gottesman, M.M., 2012. Cisplatin Resistance: A Cellular Self-Defense Mechanism Resulting from Multiple Epigenetic and Genetic Changes. *Pharmacol. Rev.* 64, 706–721. <https://doi.org/10.1124/pr.111.005637>.
- Shu, J., Silva, B.V.R.e., Gao, T., Xu, Z., Cui, J., 2017. Dynamic and Modularized MicroRNA Regulation and Its Implication in Human Cancers. *Sci. Rep.* 7, 13356. <https://doi.org/10.1038/s41598-017-13470-5>.
- Si, W., Shen, J., Zheng, H., Fan, W., 2019. The role and mechanisms of action of microRNAs in cancer drug resistance. *Clin. Epigenet.* 11, 25. <https://doi.org/10.1186/s13148-018-0587-8>.
- Siegel, R.L., Miller, K.D., Fuchs, H.E., Jemal, A., 2021. Cancer Statistics, 2021. *CA: Cancer J. Clin.* 71, 7–33. <https://doi.org/10.3322/caac.21654>.
- Singh, R., Mo, Y.-Y., 2013. Role of microRNAs in breast cancer. *Cancer Biol. Ther.* 14, 201–212. <https://doi.org/10.4161/cbt.23296>.
- Štarha, P., Trávníček, Z., Popa, I., 2010. Platinum(II) oxalato complexes with adenine-based carrier ligands showing significant in vitro antitumor activity. *J. Inorg. Biochem.* 104. <https://doi.org/10.1016/j.jinorgbio.2010.02.005>.
- Štarha, P., Vančo, J., Trávníček, Z., 2017. Platinum complexes containing adenine-based ligands: An overview of selected structural features. *Coord. Chem. Rev.* 332. <https://doi.org/10.1016/j.ccr.2016.09.017>.
- Stewart, D.J., 2007. Mechanisms of resistance to cisplatin and carboplatin. *Crit. Rev. Oncol. /Hematol.* 63, 12–31. <https://doi.org/10.1016/j.critrevonc.2007.02.001>.
- Sticht, C., De La Torre, C., Parveen, A., Gretz, N., 2018. miRWalk: An online resource for prediction of microRNA binding sites. *PLoS ONE* 13. <https://doi.org/10.1371/journal.pone.0206239> e0206239.
- Sulaiman, A.A., Alhoshani, A., As Sobeai, H.M., Alghanem, M., Abogosh, A.K., Ahmad, S., Altaf, M., Monim-ul-Mehboob, M., Stoeckli-Evans, H., Isab, A.A., 2020a. Anticancer activity and X-ray structure determination of gold(I) complexes of 2-(diphenylphosphanyl)-1-aminocyclohexane. *Polyhedron* 183. <https://doi.org/10.1016/j.poly.2020.114532> 114532.
- Sulaiman, A.A., Zierkiewicz, W., Michalczyk, M., Malik-Gajewska, M., Ahmad, S., Alhoshani, A., As Sobeai, H.M., Bieńko, D., Isab, A.A., 2020b. Synthesis, characterization, DFT optimization and anticancer evaluation of phosphane-gold(I) dithiocarbamates. *J. Mol. Struct.* 1218. <https://doi.org/10.1016/j.molstruc.2020.128486> 128486.
- Sun, Y., Hu, T., Gou, S., Cao, Z., 2012. Novel hydrophilic cis-bis(cyclopentylamine)platinum(II) complexes: Synthesis, characterization, antitumor activity and interaction with DNA. *Inorg. Chim. Acta* 391. <https://doi.org/10.1016/j.ica.2012.05.002>.
- Sung, H., Ferlay, J., Siegel, R.L., Laversanne, M., Soerjomataram, I., Jemal, A., Bray, F., 2021. Global cancer statistics 2020: GLOBOCAN estimates of incidence and mortality worldwide for 36 cancers in 185 countries. *CA: Cancer J. Clin.* CAAC.21660. <https://doi.org/10.3322/caac.21660>.
- Tamasi, G., Casolaro, M., Magnani, A., Segal, A., Chiasserini, L., Messori, L., Gabbiani, C., Valiahd, S.M., Jakupec, M.A., Keppler, B.K., Hursthouse, M.B., Cini, R., 2010. New platinum–oxicam complexes as anti-cancer drugs. Synthesis, characterization, release studies from smart hydrogels, evaluation of reactivity with selected proteins and cytotoxic activity in vitro. *J. Inorg. Biochem.* 104. <https://doi.org/10.1016/j.jinorgbio.2010.03.010>.
- Tian, W., He, L., 2015. Synthesis and anticancer activity of diam(m)ine platinum(II) complexes with 3-oxo-cyclobutane-1,1-dicarboxylate as the leaving group. *Res. Chem. Intermed.* 41. <https://doi.org/10.1007/s11164-015-1924-6>.
- Wazeer, M.I.M., Isab, A.A., Perzanowski, H.P., 2003. Solid-state NMR studies of 1,3-imidazolidine-2-selenone and some related compounds. *Magn. Reson. Chem.* 41. <https://doi.org/10.1002/mrc.1305>.
- Wheate, N.J., Walker, S., Craig, G.E., Oun, R., 2010. The status of platinum anticancer drugs in the clinic and in clinical trials. *Dalton Trans.* 39, 8113. <https://doi.org/10.1039/c0dt00292e>.
- Wilson, J.J., Lippard, S.J., 2014. Synthetic Methods for the Preparation of Platinum Anticancer Complexes. *Chem. Rev.* 114, 4470–4495. <https://doi.org/10.1021/cr4004314>.

- Wu, K.-L., Tsai, Y.-M., Lien, C.-T., Kuo, P.-L., Hung, J.-Y., 2019. The Roles of MicroRNA in Lung Cancer. *Int. J. Mol. Sci.* 20, 1611. <https://doi.org/10.3390/ijms20071611>.
- Wu, X., Piper-Hunter, M.G., Crawford, M., Nuovo, G.J., Marsh, C. B., Otterson, G.A., Nana-Sinkam, S.P., 2009. MicroRNAs in the Pathogenesis of Lung Cancer. *J. Thoracic Oncol.* 4, 1028–1034. <https://doi.org/10.1097/JTO.0b013e3181a99c77>.
- Yang, N.J., Hinner, M.J., 2015. Getting across the cell membrane: an overview for small molecules, peptides, and proteins. *Methods Mol. Biol. (Clifton N.J.)* 1266, 29–53. https://doi.org/10.1007/978-1-4939-2272-7_3.
- Yerukala Sathipati, S., Ho, S.-Y., 2017. Identifying the miRNA signature associated with survival time in patients with lung adenocarcinoma using miRNA expression profiles. *Sci. Rep.* 7, 7507. <https://doi.org/10.1038/s41598-017-07739-y>.
- Yin, R., Gou, S., Liu, X., Lou, L., 2011. Antitumor activities and interaction with DNA of oxaliplatin-type platinum complexes with linear or branched alkoxyacetates as leaving groups. *J. Inorg. Biochem.* 105. <https://doi.org/10.1016/j.jinorgbio.2011.05.005>.
- Zeng, L., Li, Y., Li, T., Cao, W., Yi, Y., Geng, W., Sun, Z., Xu, H., 2014. Selenium-Platinum Coordination Compounds as Novel Anticancer Drugs: Selectively Killing Cancer Cells via a Reactive Oxygen Species (ROS)-Mediated Apoptosis Route. *Chem. Asian J.* 9. <https://doi.org/10.1002/asia.201402256>.
- Zhong, X., Coukos, G., Zhang, L., 2012. miRNAs in Human Cancer, pp. 295–306. https://doi.org/10.1007/978-1-61779-427-8_21
- Zisowsky, J., Koegel, S., Leyers, S., Devarakonda, K., Kassack, M. U., Osmak, M., Jaehde, U., 2007. Relevance of drug uptake and efflux for cisplatin sensitivity of tumor cells. *Biochem. Pharmacol.* 73, 298–307. <https://doi.org/10.1016/j.bcp.2006.10.003>.